

Formation feedback control for multiple spacecraft via virtual structures

W. Ren and R.W. Beard

Abstract: Formation control ideas for multiple spacecraft using the virtual structure approach are presented. If there is no formation feedback from the spacecraft to the virtual structure, the spacecraft will get out of formation when the virtual structure moves too fast for the spacecraft to track due to spacecraft control saturation or the total system must sacrifice convergence speed in order to keep the spacecraft in formation. The spacecraft may also get out of formation when the system is affected by internal or external disturbances. To overcome these drawbacks, an idea of introducing formation feedback from the spacecraft to the virtual structure is illustrated in detail. An application of these ideas to multiple spacecraft interferometers in deep space is given.

1 Introduction

The coordination and control of formations of multiple vehicles has received significant attention in recent years. Applications in this area include the coordination of multiple robots, unmanned air vehicles, satellites, aircraft, autonomous underwater vehicles, and spacecraft [1–12]. Many different control strategies, schemes, and applications of multiple vehicle control have been contributed to the literature. While the applications are different, the fundamental approaches to formation control are similar: the common theme being the coordination of multiple vehicles in a certain way to accomplish an objective.

In terms of formation control approaches, to name a few, there are roughly three approaches reported in the literature, namely leader-following, behavioural, and virtual structure approaches. In the leader-following approach [1, 12–14], some agents are designated as leaders while others are designated as followers. The leaders track predefined trajectories, and the followers track transformed versions of the states of their nearest neighbours according to given schemes. One advantage of the leader-following approach is that it is easy to understand and implement. Another advantage is that the formation can still be maintained even if the leader is perturbed by some disturbances. The disadvantage is that there is no explicit feedback to the formation, that is, no explicit feedback from the followers to the leader in this case. If the follower is perturbed, the formation cannot be maintained. Another disadvantage is that the leader is a single point of failure for the formation.

In the behavioural approach [2, 15–17], the control action for each agent is defined by a weighted average of the control corresponding to each desired behaviour for the agent. Possible behaviours include collision avoidance, obstacle avoidance, goal seeking, formation keeping, and so on. One advantage of the behavioural approach is that it is

natural to derive control strategies when vehicles have multiple competing objectives. Another advantage is that explicit feedback is included through communication between neighbours. One disadvantage of the behavioural approach is that the group behaviour cannot be explicitly defined. Another disadvantage is that it is hard to analyse the behavioural approach mathematically and guarantee its group stability.

In the virtual structure approach [3, 18], the entire desired formation is treated as a single entity. The desired states for each vehicle in the formation can be specified by the placeholders in the virtual structure. Similar ideas include the perceptive reference frame in [8], the virtual leader in [19], and the formation reference point in [20]. One advantage of the virtual structure approach is that it is easy to prescribe the coordinated behaviour for the group. Another advantage is that the virtual structure can maintain the formation very well during the manoeuvres in the sense that the virtual structure can evolve as a whole in a given direction with some given orientation and maintain a rigid geometric relationship among multiple vehicles. The disadvantage is that requiring the formation to act as a virtual structure limits the class of potential applications of this approach. For example, when the formation shape is time-varying or needs to be reconfigured frequently, the virtual structure approach may not be the best option.

In the case of the application of synthesising multiple spacecraft interferometers [21] in deep space, it is desirable to have a constellation of spacecraft act as a single rigid body in order to image stars in deep space, that is, a certain tight formation shape needs to be preserved in this case. As a result, it is suitable to choose the virtual structure approach to accomplish formation manoeuvres.

In general, there is a dilemma when there is no feedback applied from the spacecraft to the virtual structure. On the one hand, if the virtual structure evolves too fast, the spacecraft cannot track their desired trajectories accurately since their control force or torque may reach saturation limits. As a result, the spacecraft will get out of formation. On the other hand, the virtual structure might be slowed down sufficiently to allow the spacecraft to track their trajectories accurately. However, this results in unreasonably slow formation dynamics. Also, when performing formation manoeuvres, the total system is often disturbed by internal or external factors. For example, some spacecraft

© IEE, 2004

IEE Proceedings online no. 20040484

doi: 10.1049/ip-cta:20040484

Paper first received 13th May 2003 and in revised form 10th February 2004

The authors are with the Department of Electrical and Computer Engineering, Brigham Young University, Provo, Utah 84602, USA

may disintegrate from the formation due to external disturbances in deep space or may even fail for a period of time due to mechanical or electrical malfunctions. If there is no feedback from spacecraft to the formation, the disintegrated or failed spacecraft will be left behind while the other spacecraft still keep moving towards their final goals, and the entire system cannot adjust to maintain formation. In the remainder of the paper, we refer to the group feedback from vehicles to the formation as formation feedback. Formation feedback from spacecraft to the virtual structure provides a good compromise between formation keeping and convergence speed as well as improved group stability and robustness.

The idea of formation feedback is brought to the literature recently in [6, 18, 22, 23]. In [18], the authors introduce a coordination architecture for spacecraft formation control which subsumes leader-following, behavioural, and virtual structure approaches to the multi-agent coordination problem. Using this architecture, including formation feedback is possible but it is not implemented in the paper. In [22], formation feedback is used for the coordinated control problem for multiple robots. In the case of spacecraft control, system dynamics are more complicated than the double integrator dynamics applied in [22]. In [6], a Lyapunov formation function is used to define a formation error for a class of robots (double integrator dynamics) so that a constrained motion control problem of multiple systems is converted into a stabilisation problem for one single system. In [6], error feedback is incorporated to the virtual leader through parameterised trajectories. The strength of this approach is that the formation error is guaranteed to be below a given upperbound under certain assumptions. However, this approach results in a steady-state formation error during the manoeuvre, that is, the formation error will always reach an equilibrium value which is close to the given upperbound even if the initial formation error is zero. As a result, formation is only maintained within a certain bound during the manoeuvre, which may not be proper for the requirement of precise formation maintenance.

This paper is aimed as a further development of [18] and [22]. We will propose a different approach of formation feedback from [6] and apply this idea to the more complicated spacecraft interferometry problem so that formation keeping is guaranteed throughout the manoeuvre and the total system robustness is improved. The main features of our approach are as follows. Firstly, the approach is easy to implement. The formation feedback is included through a non-linear gain matrix in the virtual structure dynamics. The components of this matrix can be conveniently tuned to satisfy different design specifications. Secondly, the approach guarantees both formation maintenance and formation speed. Using coupled dynamics between each spacecraft and the virtual structure, the system will achieve a reasonable speed based on current formation maintenance level. During the manoeuvre, tracking error for each spacecraft will approach zero, that is, spacecraft will preserve the desired formation shape precisely. When the formation is maintained accurately, the formation can evolve at a reasonably fast speed and keep this speed. Thirdly, detailed simulation analyses are provided to consider the cases of control saturation and disturbances. The system with formation feedback preserves the formation much better than the system without formation feedback. It is worthwhile to mention that the same idea proposed in this paper is also applicable to the leader-following approach except that in that case, the formation feedback is introduced from the followers to the leader.

2 Background and problem statement

In the virtual structure approach, we treat the entire desired formation as a single entity with place-holders corresponding to each spacecraft embedded in the virtual structure to represent the desired position and attitude for each spacecraft. As the virtual structure, that is, the entire desired formation as a whole evolves in time, the place-holders trace out trajectories for each corresponding spacecraft to track.

The coordinate frame geometry is shown in Fig. 1. Reference frame C_O is an inertial frame. Reference frame C_i is embedded in the i th spacecraft as a body frame to represent its configuration. Reference frame C_i^d is embedded in the i th place-holder to represent the i th spacecraft's desired configuration. The desired formation shape can then be defined by the relative geometric configuration among place-holders, that is, among desired reference frame C_i^d . Since the desired formation can be thought of as a single entity with inertial position \mathbf{r}_F , velocity \mathbf{v}_F , unit quaternion attitude \mathbf{q}_F , and angular velocity $\boldsymbol{\omega}_F$, we define the formation reference frame C_F located at \mathbf{r}_F , which is also the virtual centre of the virtual structure, with an orientation given by \mathbf{q}_F with respect to the inertial frame C_O . Each spacecraft can be represented either by position \mathbf{r}_i , velocity \mathbf{v}_i , unit quaternion attitude \mathbf{q}_i , and angular velocity $\boldsymbol{\omega}_i$ with respect to the inertial frame C_O or, by \mathbf{r}_{iF} , \mathbf{v}_{iF} , \mathbf{q}_{iF} , and $\boldsymbol{\omega}_{iF}$ with respect to the formation reference frame C_F . Correspondingly, a superscript 'd' above a vector represents the desired state for each spacecraft, that is, the actual state for each corresponding place-holder. For simplicity, we use the same symbol to denote a vector and its corresponding coordinate frame representation in the remainder of the paper.

In this paper, the control is derived in four steps: firstly, the dynamics of the virtual structure are defined; secondly, the motion of the virtual structure is translated into the desired motion for each spacecraft; thirdly, tracking controls for each spacecraft are derived; and finally, formation feedback is introduced from each spacecraft to the virtual structure.

In the sequel, we will first introduce spacecraft dynamics. Then, the desired states for each spacecraft will be derived from the states of the virtual structure. Finally, we define the dynamics of the virtual structure.

2.1 Spacecraft dynamics

The translational dynamics for the i th spacecraft are

$$\begin{aligned} \dot{\mathbf{r}}_i &= \mathbf{v}_i \\ M_i \dot{\mathbf{v}}_i &= \mathbf{f}_i \end{aligned} \quad (1)$$

where M_i is the mass of the i th spacecraft, and \mathbf{f}_i is the control force.

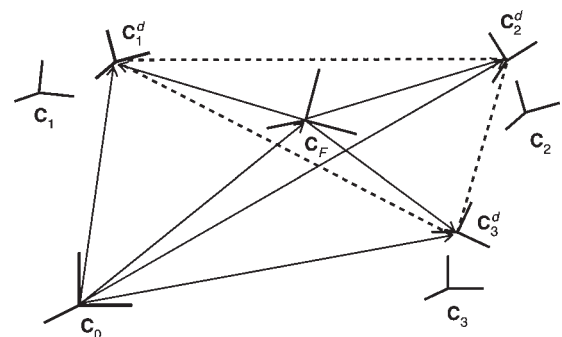


Fig. 1 Coordinate frame geometry

The rotational dynamics for the i th spacecraft [24] are

$$\begin{aligned}\dot{\bar{\mathbf{q}}}_i &= -\frac{1}{2}\boldsymbol{\omega}_i \times \bar{\mathbf{q}}_i + \frac{1}{2}\bar{q}_i\boldsymbol{\omega}_i \\ \dot{q}_i &= -\frac{1}{2}\boldsymbol{\omega}_i \cdot \bar{\mathbf{q}}_i \\ \mathbf{J}_i\dot{\boldsymbol{\omega}}_i &= -\boldsymbol{\omega}_i \times \mathbf{J}_i\boldsymbol{\omega}_i + \boldsymbol{\tau}_i\end{aligned}\quad (2)$$

where $\bar{\mathbf{q}}_i$ is the vector part of the quaternion \mathbf{q}_i , \bar{q}_i is the scalar part of the quaternion \mathbf{q}_i (see Appendix), \mathbf{J}_i is the moment of inertia of the i th spacecraft, and $\boldsymbol{\tau}_i$ is the control torque on the i th spacecraft.

2.2 Desired states for each spacecraft

The desired states for the i th spacecraft in terms of its corresponding coordinate representation are given by

$$\begin{aligned}\mathbf{r}_i^d(t) &= \mathbf{r}_F(t) + \mathbf{C}_{OF}(t)\mathbf{r}_{iF}^d(t) \\ \mathbf{v}_i^d(t) &= \mathbf{v}_F(t) + \mathbf{C}_{OF}(t)\mathbf{v}_{iF}^d(t) \\ &\quad + \boldsymbol{\omega}_F(t) \times (\mathbf{C}_{OF}(t)\mathbf{r}_{iF}^d(t)) \\ \mathbf{q}_i^d(t) &= \mathbf{q}_F(t)\mathbf{q}_{iF}^d(t) \\ \boldsymbol{\omega}_i^d(t) &= \boldsymbol{\omega}_F(t) + \mathbf{C}_{OF}(t)\boldsymbol{\omega}_{iF}^d(t)\end{aligned}\quad (3)$$

where $\mathbf{C}_{OF}(t)$ is the rotation matrix of the frame \mathbf{C}_O with respect to \mathbf{C}_F . \mathbf{C}_{OF} is given as

$$\mathbf{C}_{OF} = \mathbf{C}_{FO}^T = (2\bar{q}_F^2 - 1)\mathbf{I} + 2\bar{\mathbf{q}}_F\bar{q}_F^T + 2\bar{q}_F\bar{\mathbf{q}}_F^\times$$

Generally, all parameters in (3) can vary with time. Among them, \mathbf{r}_F and \mathbf{v}_F correspond to the translational motion of the virtual structure, \mathbf{q}_F , $\boldsymbol{\omega}_F$, and \mathbf{C}_{OF} correspond to the rotational motion of the virtual structure, and \mathbf{r}_{iF}^d , \mathbf{v}_{iF}^d , \mathbf{q}_{iF}^d , and $\boldsymbol{\omega}_{iF}^d$ correspond to the desired formation shape. Therefore, if \mathbf{r}_{iF}^d , \mathbf{q}_{iF}^d , \mathbf{v}_{iF}^d , and $\boldsymbol{\omega}_{iF}^d$ vary with time, the desired formation shape is time-varying. However, if we are concerned with formation manoeuvres that preserve the overall formation shape, that is, each place-holder needs to preserve fixed relative position and orientation in the virtual structure, \mathbf{r}_{iF}^d and \mathbf{v}_{iF}^d should be constant and \mathbf{q}_{iF}^d and $\boldsymbol{\omega}_{iF}^d$ should be zero. The requirement to preserve fixed relative position between each place-holder in the virtual structure can be loosened to make the formation shape more flexible by allowing the place-holders to expand or contract while still keeping fixed relative orientation, that is, the overall formation shape is allowed to be expanded or contracted. In this paper, we focus on formation manoeuvres that have those properties. Of course, the approach hereafter can easily be extended to the general case.

Group manoeuvres with the above properties can be achieved as a succession of elementary formation manoeuvres. Therefore, we will redefine the desired states for each spacecraft via elementary formation manoeuvres. The elementary formation manoeuvres include translations, rotations, and expansions/contractions. Let $\boldsymbol{\xi}_F(t) = [\xi_1(t), \xi_2(t), \xi_3(t)]^T$ with its components representing the expansion/contraction rates along each \mathbf{C}_F axis. An expansion/contraction matrix is defined as $\boldsymbol{\Xi}(t) = \text{diag}(\boldsymbol{\xi}_F(t))$, which is a diagonal matrix. The coordination vector can then be defined as $\mathbf{X}_F(t) = [\mathbf{r}_F^T, \mathbf{v}_F^T, \mathbf{q}_F^T, \boldsymbol{\omega}_F^T, \boldsymbol{\xi}_F^T, \boldsymbol{\xi}_F^T]^T$, which represents the states of the virtual structure with respect to the inertial frame \mathbf{C}_O .

To realise elementary formation manoeuvres, we can vary \mathbf{r}_F and \mathbf{v}_F to translate the formation, vary \mathbf{q}_F (\mathbf{q}_F can be transformed to the rotation matrix \mathbf{C}_{OF} .) and $\boldsymbol{\omega}_F$ to rotate the formation, and vary $\boldsymbol{\xi}_F$ and $\boldsymbol{\xi}_F$ to expand/contract the formation. Arbitrary formation manoeuvres can be realised

by varying $\mathbf{r}_F(t)$, $\mathbf{v}_F(t)$, $\mathbf{q}_F(t)$, $\boldsymbol{\omega}_F(t)$, $\boldsymbol{\xi}(t)$, and $\boldsymbol{\xi}(t)$ simultaneously. As a result, the desired states for the i th spacecraft are redefined as

$$\begin{aligned}\mathbf{r}_i^d(t) &= \mathbf{r}_F(t) + \mathbf{C}_{OF}(t)\boldsymbol{\Xi}(t)\mathbf{r}_{iF}^d \\ \mathbf{v}_i^d(t) &= \mathbf{v}_F(t) + \mathbf{C}_{OF}(t)\boldsymbol{\Xi}(t)\mathbf{v}_{iF}^d \\ &\quad + \boldsymbol{\omega}_F(t) \times (\mathbf{C}_{OF}(t)\boldsymbol{\Xi}(t)\mathbf{r}_{iF}^d) \\ \mathbf{q}_i^d(t) &= \mathbf{q}_F(t)\mathbf{q}_{iF}^d \\ \boldsymbol{\omega}_i^d(t) &= \boldsymbol{\omega}_F(t)\end{aligned}\quad (4)$$

Obviously, assuming that \mathbf{r}_{iF}^d and \mathbf{q}_{iF}^d are given in advance of the desired formation shape specifications, the desired states for each spacecraft are determined by the states of the virtual structure, that is, the coordination vector \mathbf{X}_F .

The derivatives of the desired states are given by

$$\begin{aligned}\dot{\mathbf{r}}_i^d(t) &= \dot{\mathbf{r}}_F(t) + \boldsymbol{\omega}_F \times (\mathbf{C}_{OF}(t)\boldsymbol{\Xi}(t)\mathbf{r}_{iF}^d) + \mathbf{C}_{OF}(t)\dot{\boldsymbol{\Xi}}(t)\mathbf{r}_{iF}^d \\ \dot{\mathbf{v}}_i^d(t) &= \dot{\mathbf{v}}_F(t) + 2\boldsymbol{\omega}_F \times (\mathbf{C}_{OF}(t)\boldsymbol{\Xi}(t)\mathbf{r}_{iF}^d) \\ &\quad + \mathbf{C}_{OF}(t)\dot{\boldsymbol{\Xi}}(t)\mathbf{r}_{iF}^d + \dot{\boldsymbol{\omega}}_F(t) \times (\mathbf{C}_{OF}(t)\boldsymbol{\Xi}(t)\mathbf{r}_{iF}^d) \\ \dot{\mathbf{q}}_i^d(t) &= \dot{\mathbf{q}}_F(t)\mathbf{q}_{iF}^d \\ \dot{\boldsymbol{\omega}}_i^d(t) &= \dot{\boldsymbol{\omega}}_F(t)\end{aligned}\quad (5)$$

From (4), we can see that if the velocity of the formation is zero, that is, $\mathbf{v}_F(t) = 0$, $\boldsymbol{\omega}_F(t) = 0$, and $\dot{\boldsymbol{\xi}}(t) = 0$, then the desired velocity of each spacecraft is zero, that is, $\mathbf{v}_i^d(t) = 0$ and $\boldsymbol{\omega}_i^d(t) = 0$. Also, from (4) and (5), if both the velocity and acceleration of the formation are zero, that is, $\mathbf{v}_F(t) = 0$, $\boldsymbol{\omega}_F(t) = 0$, $\dot{\boldsymbol{\xi}}(t) = 0$, $\dot{\mathbf{v}}_F(t) = 0$, $\dot{\boldsymbol{\omega}}_F(t) = 0$, and $\dot{\boldsymbol{\xi}}(t) = 0$, then both the desired velocity and acceleration of each spacecraft are zero, that is, $\mathbf{v}_i^d(t) = 0$, $\boldsymbol{\omega}_i^d(t) = 0$, $\dot{\mathbf{v}}_i^d(t) = 0$, and $\dot{\boldsymbol{\omega}}_i^d(t) = 0$.

2.3 Dynamics of the virtual structure

Since the virtual structure is thought of as a rigid body, we assume that its actual and desired states, that is, the coordination vector \mathbf{X}_F and desired coordination vector \mathbf{X}_F^d , both satisfy the following rigid body dynamics

$$\begin{pmatrix} \dot{\mathbf{r}}_F \\ M_F\dot{\mathbf{v}}_F \\ \dot{\bar{\mathbf{q}}}_F \\ \dot{q}_F \\ \mathbf{J}_F\dot{\boldsymbol{\omega}}_F \\ \dot{\boldsymbol{\xi}}_F \\ \dot{\boldsymbol{\xi}}_F \end{pmatrix} = \begin{pmatrix} \mathbf{v}_F \\ \mathbf{f}_F \\ -\frac{1}{2}\boldsymbol{\omega}_F \times \bar{\mathbf{q}}_F + \frac{1}{2}\bar{q}_F\boldsymbol{\omega}_F \\ -\frac{1}{2}\boldsymbol{\omega}_F \cdot \bar{\mathbf{q}}_F \\ -\boldsymbol{\omega}_F \times \mathbf{J}_F\boldsymbol{\omega}_F + \boldsymbol{\tau}_F \\ \boldsymbol{\xi}_F \\ \boldsymbol{\nu}_F \end{pmatrix}\quad (6)$$

where M_F and \mathbf{J}_F are the virtual mass and virtual inertia of the virtual structure, \mathbf{f}_F and $\boldsymbol{\tau}_F$ are the virtual force and virtual torque exerted on the virtual structure, and $\boldsymbol{\nu}_F$ is the virtual control effort used to expand or contract the formation.

Unlike spacecraft dynamics, the virtual structure dynamics is implemented on-board. As a result, there are no physical saturation constraints for its control effort. Also, the virtual mass and inertia can be chosen arbitrarily based on the design requirements. Intuitively, controls with fast performance and high cost may be implemented easily. However, as we will see later, the control law design for the virtual structure affects system formation maintenance significantly.

3 Formation control strategies with formation feedback

In this section we propose control strategies for both virtual structure dynamics and spacecraft dynamics. Formation feedback will be introduced from the spacecraft to the virtual structure.

3.1 Main results

Let $\mathbf{X}_i(t) = [\mathbf{r}_i^T, \mathbf{v}_i^T, \mathbf{q}_i^T, \boldsymbol{\omega}_i^T]^T$ and $\mathbf{X}_i^d(t) = [\mathbf{r}_i^{dT}, \mathbf{v}_i^{dT}, \mathbf{q}_i^{dT}, \boldsymbol{\omega}_i^{dT}]^T$ represent the states and desired states for the i th spacecraft with respect to the inertial frame \mathbf{C}_O respectively. Accordingly, let $\mathbf{X} = [\mathbf{X}_1^T, \mathbf{X}_2^T, \dots, \mathbf{X}_N^T]^T$ and $\mathbf{X}^d = [\mathbf{X}_1^{dT}, \mathbf{X}_2^{dT}, \dots, \mathbf{X}_N^{dT}]^T$, where N is the number of spacecraft in the formation. Let $\mathbf{X}_F(t)$ be the coordination vector defined in Section 2 and $\mathbf{X}_F^d = [\mathbf{r}_F^d, \mathbf{v}_F^d, \mathbf{q}_F^d, \boldsymbol{\omega}_F^d, \boldsymbol{\xi}_F^d, \tilde{\boldsymbol{\xi}}_F^d]^T$ be the desired constant coordination vector. Unlike \mathbf{r}_i^d and \mathbf{q}_i^d , \mathbf{r}_F^d , \mathbf{q}_F^d , and $\boldsymbol{\xi}_F^d$ are constant, which implies that $\mathbf{v}_F^d = \boldsymbol{\omega}_F^d = \tilde{\boldsymbol{\xi}}_F^d = 0$. Hereafter, we use a tilde above a vector to represent the error state between the actual state and the desired state, e.g. $\tilde{\mathbf{r}}_i = \mathbf{r}_i - \mathbf{r}_i^d$, $\tilde{\mathbf{q}}_i = \mathbf{q}_i - \mathbf{q}_i^d$, and so on.

The aim of the formation manoeuvre is to drive $\mathbf{X}_F(t)$ to \mathbf{X}_F^d while guaranteeing that $\mathbf{X}_i(t)$ tracks $\mathbf{X}_i^d(t)$. Accordingly, we have the following definition.

Definition 3.1: A formation manoeuvre is asymptotically achieved if $\mathbf{X}_F(t) \rightarrow \mathbf{X}_F^d$ and $\mathbf{X}_i(t) \rightarrow \mathbf{X}_i^d(t)$ as $t \rightarrow \infty$.

A centralised scheme will be used to illustrate the idea of introducing formation feedback from spacecraft to the virtual structure since only a few spacecraft are involved in the application example. In the case of decentralised control implementation of the virtual structure approach, a similar idea can also be applied. Therefore, one strategy is that the coordination vector \mathbf{X}_F can be implemented at a centralised location (e.g. one of the spacecraft) and broadcast to each spacecraft. Accordingly, each spacecraft can derive its desired states $\mathbf{X}_i^d(t)$ from \mathbf{X}_F following (4). Another strategy is that the desired states for each spacecraft can be implemented at the same location as the coordination vector, and then the desired states can be transmitted to each corresponding spacecraft respectively. Obviously the second strategy introduces more computation and communication requirement to the centralised location than the first one but it is suitable for time-varying formation shape. In this paper, we apply the first strategy.

The following lemma, known as the Rayleigh-Ritz Theorem will be used to analyse our result.

Lemma 3.1: If $\mathbf{A} \in \mathbb{R}^{n \times n}$ is symmetric, and $\underline{\lambda}(\mathbf{A})$ and $\bar{\lambda}(\mathbf{A})$ are the smallest and largest eigenvalue of \mathbf{A} respectively, then

$$\underline{\lambda}(\mathbf{A})\mathbf{x}^T\mathbf{x} \leq \mathbf{x}^T\mathbf{A}\mathbf{x} \leq \bar{\lambda}(\mathbf{A})\mathbf{x}^T\mathbf{x}, \quad \forall \mathbf{x} \in \mathbb{R}^n$$

$$\underline{\lambda}(\mathbf{A}) = \min \frac{\mathbf{x}^T\mathbf{A}\mathbf{x}}{\mathbf{x}^T\mathbf{x}}, \quad \forall \mathbf{x} \neq 0$$

$$\bar{\lambda}(\mathbf{A}) = \max \frac{\mathbf{x}^T\mathbf{A}\mathbf{x}}{\mathbf{x}^T\mathbf{x}}, \quad \forall \mathbf{x} \neq 0$$

Proof: see [25]. \square

We have the following theorem to guarantee that a formation manoeuvre is asymptotically achieved with formation feedback.

Theorem 3.2: Let

$$\begin{pmatrix} \dot{\mathbf{r}}_F \\ \dot{\mathbf{v}}_F \\ \dot{\tilde{\mathbf{q}}}_F \\ \dot{\tilde{\mathbf{q}}}_F \\ \mathbf{J}_F \dot{\boldsymbol{\omega}}_F \\ \dot{\boldsymbol{\xi}}_F \\ \dot{\tilde{\boldsymbol{\xi}}}_F \end{pmatrix} = \begin{pmatrix} \mathbf{v}_F \\ -\mathbf{K}_r(\mathbf{r}_F - \mathbf{r}_F^d) - \Gamma_v(\mathbf{X}, \mathbf{X}^d)\mathbf{v}_F \\ -k_p\|\mathbf{r}_F - \mathbf{r}_F^d\|^2\mathbf{v}_F/\|\mathbf{v}_F\|^2 \\ -\frac{1}{2}\boldsymbol{\omega}_F \times \tilde{\mathbf{q}}_F + \frac{1}{2}\tilde{\mathbf{q}}_F\boldsymbol{\omega}_F \\ -\frac{1}{2}\boldsymbol{\omega}_F \cdot \tilde{\mathbf{q}}_F \\ -\boldsymbol{\omega}_F \times \mathbf{J}_F\boldsymbol{\omega}_F + k_q\tilde{\mathbf{q}}_e\mathbf{F} - \Gamma_\omega(\mathbf{X}, \mathbf{X}^d)\boldsymbol{\omega}_F \\ -k_a\|\mathbf{q}_F - \mathbf{q}_F^d\|^2\boldsymbol{\omega}_F/\|\boldsymbol{\omega}_F\|^2 \\ \tilde{\boldsymbol{\xi}}_F \\ -\mathbf{K}_\xi(\boldsymbol{\xi}_F - \boldsymbol{\xi}_F^d) - \Gamma_\xi(\mathbf{X}, \mathbf{X}^d)\boldsymbol{\xi}_F \\ -k_e\|\boldsymbol{\xi}_F - \boldsymbol{\xi}_F^d\|^2\boldsymbol{\xi}_F/\|\boldsymbol{\xi}_F\|^2 \end{pmatrix} \quad (7)$$

and

$$\begin{pmatrix} \dot{\mathbf{r}}_i \\ \dot{\mathbf{v}}_i \\ \dot{\tilde{\mathbf{q}}}_i \\ \dot{\tilde{\mathbf{q}}}_i \\ \mathbf{J}_i \dot{\boldsymbol{\omega}}_i \end{pmatrix} = \begin{pmatrix} \mathbf{v}_i \\ \mathbf{v}_i^d - \mathbf{K}_{ri}(\mathbf{r}_i - \mathbf{r}_i^d) - \mathbf{K}_{vi}(\mathbf{v}_i - \mathbf{v}_i^d) \\ -\frac{1}{2}\boldsymbol{\omega}_i \times \tilde{\mathbf{q}}_i + \frac{1}{2}\tilde{\mathbf{q}}_i\boldsymbol{\omega}_i \\ -\frac{1}{2}\boldsymbol{\omega}_i \cdot \tilde{\mathbf{q}}_i \\ -\boldsymbol{\omega}_i \times \mathbf{J}_i\boldsymbol{\omega}_i + \mathbf{J}_i\boldsymbol{\omega}_i^d + \frac{1}{2}\boldsymbol{\omega}_i \times \mathbf{J}_i(\boldsymbol{\omega}_i + \boldsymbol{\omega}_i^d) \\ +k_{qi}\tilde{\mathbf{q}}_e\mathbf{i} - \mathbf{K}_{oi}(\boldsymbol{\omega}_i - \boldsymbol{\omega}_i^d) \end{pmatrix} \quad (8)$$

If \mathbf{K}_r , \mathbf{K}_ξ , \mathbf{K}_{ri} , \mathbf{K}_{vi} , and \mathbf{K}_{oi} are symmetric positive definite matrices, k_p , k_a , and k_e are non-negative scalars, k_q and k_{qi} are positive scalars, $\Gamma_v(\mathbf{X}, \mathbf{X}^d)$, $\Gamma_\omega(\mathbf{X}, \mathbf{X}^d)$, and $\Gamma_\xi(\mathbf{X}, \mathbf{X}^d)$ are symmetric positive definite matrices with entries continuously dependent on \mathbf{X} and \mathbf{X}^d , and $\mathbf{q}_{eF} = \mathbf{q}_F^*\mathbf{q}_F^d$ and $\mathbf{q}_{ei} = \mathbf{q}_i^*\mathbf{q}_i^d$, then $\|\mathbf{X}_F(t) - \mathbf{X}_F^d\| \rightarrow 0$ and $\|\mathbf{X}_i(t) - \mathbf{X}_i^d(t)\| \rightarrow 0$ as $t \rightarrow \infty$.

Proof: With formation feedback, the spacecraft dynamics (8) and the virtual structure dynamics (7) are coupled in the sense that each spacecraft needs the virtual structure states \mathbf{X}_F to specify its desired states \mathbf{X}_i^d according to (4) while the virtual structure needs spacecraft states \mathbf{X} to include formation feedback. The spacecraft control law (8) can be thought of as $\dot{\tilde{\mathbf{X}}}_i = f(\tilde{\mathbf{X}}_i, \mathbf{X}_F)$ and the virtual structure control law (7) can be thought of as $\dot{\tilde{\mathbf{X}}}_F = g(\tilde{\mathbf{X}}_F, \mathbf{X}_F)$, where $f(\cdot, \cdot)$ and $g(\cdot, \cdot)$ can be specified from each control law. Therefore, the coupled dynamics are time-invariant with states $\tilde{\mathbf{X}}$ and \mathbf{X}_F , which means that LaSalle's invariance principle is valid.

Consider a Lyapunov function candidate

$$V = V_F + \sum_{i=1}^N V_i$$

where

$$V_F = \frac{1}{2}\tilde{\mathbf{r}}_F^T\mathbf{K}_r\tilde{\mathbf{r}}_F + \frac{1}{2}\|\mathbf{v}_F\|^2 + k_p\|\tilde{\mathbf{q}}_F\|^2 \\ + \frac{1}{2}\boldsymbol{\omega}_F^T\mathbf{J}_F\boldsymbol{\omega}_F + \frac{1}{2}\tilde{\boldsymbol{\xi}}_F^T\mathbf{K}_\xi\tilde{\boldsymbol{\xi}}_F + \frac{1}{2}\|\tilde{\boldsymbol{\xi}}_F\|^2$$

and

$$V_i = \frac{1}{2}\tilde{\mathbf{r}}_i^T\mathbf{K}_{ri}\tilde{\mathbf{r}}_i + \frac{1}{2}\|\tilde{\mathbf{v}}_i\|^2 + k_{qi}\|\tilde{\mathbf{q}}_i\|^2 + \frac{1}{2}\tilde{\boldsymbol{\omega}}_i^T\mathbf{J}_i\tilde{\boldsymbol{\omega}}_i.$$

After some manipulation, the derivative of \mathbf{v}_F is given by:

$$\begin{aligned}\dot{V}_F = & -\mathbf{v}_F^T \Gamma_v(\mathbf{X}, \mathbf{X}^d) \mathbf{v}_F - k_p \|\tilde{\mathbf{r}}_F\|^2 \\ & - \boldsymbol{\omega}_F^T \Gamma_\omega(\mathbf{X}, \mathbf{X}^d) \boldsymbol{\omega}_F - k_a \|\tilde{\mathbf{q}}_F\|^2 \\ & - \dot{\boldsymbol{\xi}}_F^T \Gamma_\xi(\mathbf{X}, \mathbf{X}^d) \dot{\boldsymbol{\xi}}_F - k_e \|\tilde{\boldsymbol{\xi}}_F\|^2 \leq 0\end{aligned}$$

The third and fourth terms above come from the derivative of $k_q \|\tilde{\mathbf{q}}_F\|^2 + \frac{1}{2} \boldsymbol{\omega}_F^T \mathbf{J}_F \boldsymbol{\omega}_F$, which can be obtained by following a similar proof for attitude control in [12].

In the virtual structure approach, the desired states for each spacecraft also satisfy the translational dynamics (1) and rotational dynamics (2) since the desired states for each spacecraft are also the states for each corresponding placeholder in the virtual structure. Based on this fact, after some manipulation, the derivative of V_i is given by:

$$\dot{V}_i = -\tilde{\mathbf{v}}_i^T \mathbf{K}_{vi} \tilde{\mathbf{v}}_i - \tilde{\boldsymbol{\omega}}_i^T \mathbf{K}_{oi} \tilde{\boldsymbol{\omega}}_i \leq 0$$

Similarly, the second term above comes from the derivative of $k_q \|\tilde{\mathbf{q}}_i\|^2 + \frac{1}{2} \boldsymbol{\omega}_i^T \mathbf{J}_i \boldsymbol{\omega}_i$, which can also be obtained by following a similar proof for attitude control in [12].

Thus $\dot{V} = \dot{V}_F + \sum_{i=1}^N \dot{V}_i \leq 0$. Let $\Omega = \{(\tilde{\mathbf{X}}, \mathbf{X}_F) | \dot{V} = 0\}$, and let $\tilde{\Omega}$ be the largest invariant set in Ω . On $\tilde{\Omega}$, $\dot{V} \equiv 0$, which implies that $\dot{V}_F \equiv 0$ and $\dot{V}_i \equiv 0$. Two cases will be considered as follows:

Case 1: $k_p, k_a, k_e > 0$.

From $\dot{V}_F \equiv 0$, we know that $\tilde{\mathbf{r}}_F = 0$, $\mathbf{v}_F = 0$, $\tilde{\mathbf{q}}_F = 0$, $\boldsymbol{\omega}_F = 0$, $\tilde{\boldsymbol{\xi}}_F = 0$, and $\dot{\boldsymbol{\xi}}_F = 0$.

Case 2: $k_p = k_a = k_e = 0$.

From $\dot{V}_F \equiv 0$, we know that $\mathbf{v}_F = 0$, $\boldsymbol{\omega}_F = 0$, and $\dot{\boldsymbol{\xi}}_F = 0$. From $\sum_{i=1}^N \dot{V}_i \equiv 0$ and $\dot{V}_F \equiv 0$, we know that $\|\tilde{\mathbf{X}}\|$ and $\|\mathbf{X}_F\|$ are bounded, which implies that each entry in $\Gamma_v(\mathbf{X}, \mathbf{X}^d)$, $\Gamma_\omega(\mathbf{X}, \mathbf{X}^d)$, and $\Gamma_\xi(\mathbf{X}, \mathbf{X}^d)$ are also bounded. Then, from the second, fourth, and sixth equation in (7), we know that $\mathbf{r}_F = \mathbf{r}_F^d$, $\tilde{\mathbf{q}}_{eF} = 0$, which implies that $\mathbf{q}_F = \mathbf{q}_F^d$, and $\boldsymbol{\xi}_F = \boldsymbol{\xi}_F^d$.

Accordingly, from $\dot{V}_i \equiv 0$, we know that $\tilde{\mathbf{v}}_i = 0$ and $\tilde{\boldsymbol{\omega}}_i = 0$. Then, from the second and fourth equation in (8), we know that $\tilde{\mathbf{r}}_i = 0$ and $\tilde{\mathbf{q}}_{ei} = 0$, which implies that $\mathbf{q}_i = \mathbf{q}_i^d$.

Therefore, by LaSalle's invariance principle, $\|\mathbf{X}_F(t) - \mathbf{X}_F^d\| \rightarrow 0$ and $\|\mathbf{X}_i(t) - \mathbf{X}_i^d(t)\| \rightarrow 0$ asymptotically. \square

Note that if we define a translational tracking error as $E_{ii} = \frac{1}{2} \tilde{\mathbf{r}}_i^T \mathbf{K}_{ri} \tilde{\mathbf{r}}_i + \frac{1}{2} \|\tilde{\mathbf{v}}_i\|^2$, E_{ii} decreases during the manoeuvre and $\tilde{\mathbf{r}}_i^T \mathbf{K}_{ri} \tilde{\mathbf{r}}_i$ is bounded by $2E_{ii}(0) - \|\tilde{\mathbf{v}}_i\|^2$. Similarly, if we define a rotational tracking error as $E_{ri} = k_{qi} \|\tilde{\mathbf{q}}_i\|^2 + \frac{1}{2} \tilde{\boldsymbol{\omega}}_i^T \mathbf{J}_i \tilde{\boldsymbol{\omega}}_i$, E_{ri} decreases during the manoeuvre and $\|\tilde{\mathbf{q}}_i\|^2$ is bounded by $\frac{1}{k_{qi}} (E_{ri}(0) - \frac{1}{2} \tilde{\boldsymbol{\omega}}_i^T \mathbf{J}_i \tilde{\boldsymbol{\omega}}_i)$.

Corollary 3.3: If $k_p, k_a, k_e > 0$, then V_F converges to zero exponentially.

Proof: Following Lemma 3.1, it can be shown that:

$$\begin{aligned}-\mathbf{v}_F^T \Gamma_v(\mathbf{X}, \mathbf{X}^d) \mathbf{v}_F & \leq -\underline{\lambda}(\Gamma_v(\mathbf{X}, \mathbf{X}^d)) \|\mathbf{v}_F\|^2 \\ -k_p \|\tilde{\mathbf{r}}_F\|^2 & \leq -(k_p / \bar{\lambda}(\mathbf{K}_r)) \tilde{\mathbf{r}}_F^T \mathbf{K}_r \tilde{\mathbf{r}}_F \\ -\boldsymbol{\omega}_F^T \Gamma_\omega(\mathbf{X}, \mathbf{X}^d) \boldsymbol{\omega}_F & \leq -(\underline{\lambda}(\Gamma_\omega(\mathbf{X}, \mathbf{X}^d)) / \bar{\lambda}(\mathbf{J}_F)) \boldsymbol{\omega}_F^T \mathbf{J}_F \boldsymbol{\omega}_F \\ -\dot{\boldsymbol{\xi}}_F^T \Gamma_\xi(\mathbf{X}, \mathbf{X}^d) \dot{\boldsymbol{\xi}}_F & \leq -\underline{\lambda}(\Gamma_\xi(\mathbf{X}, \mathbf{X}^d)) \|\dot{\boldsymbol{\xi}}_F\|^2 \\ -k_e \|\tilde{\boldsymbol{\xi}}_F\|^2 & \leq -(k_e / \bar{\lambda}(\mathbf{K}_\xi)) \tilde{\boldsymbol{\xi}}_F^T \mathbf{K}_\xi \tilde{\boldsymbol{\xi}}_F\end{aligned}$$

Let

$$\alpha = \min\{2\underline{\lambda}(\Gamma_v(\mathbf{X}, \mathbf{X}^d)), 2k_p / \bar{\lambda}(\mathbf{K}_r), 2\underline{\lambda}(\Gamma_\omega(\mathbf{X}, \mathbf{X}^d)) / \bar{\lambda}(\mathbf{J}_F), k_e / k_q, 2\underline{\lambda}(\Gamma_\xi(\mathbf{X}, \mathbf{X}^d)), 2k_e / \bar{\lambda}(\mathbf{K}_\xi)\}$$

We know that $\dot{V}_F \leq -\alpha V_F$. Therefore, V_F converges to zero exponentially.

Remark 3.4: Note that from (7), in the case of $k_p, k_a, k_e \neq 0$, the control force, control torque, and control effort for the virtual structure may be very large when \mathbf{v}_F , $\boldsymbol{\omega}_F$, and $\dot{\boldsymbol{\xi}}_F$ approach zero. As a result, the global exponential convergence of V_F is only achieved when $\mathbf{v}_F, \boldsymbol{\omega}_F, \dot{\boldsymbol{\xi}}_F \neq 0$. Those large magnitudes can be mitigated by adding a small constant δ to each denominator in (7). Also note that unlike spacecraft dynamics, those large magnitudes may not be so undesirable for the virtual structure since the virtual structure dynamics are implemented on-board.

From (7), we can see that formation feedback is introduced from each spacecraft to the virtual structure via the non-linear gain matrix Γ_v , Γ_ω , and Γ_ξ , which depend on each spacecraft's actual and desired states. Next, we will show the design motivation and methodology of the non-linear and linear gain matrices in (7) and (8).

Define a performance measure as $E(\mathbf{X}, \mathbf{X}^d)$, which is a non-negative function of \mathbf{X} and \mathbf{X}^d and is used to measure formation maintenance. For example, $E(\mathbf{X}, \mathbf{X}^d)$ can be composed of two parts. One part is the spacecraft tracking error, i.e. $\tilde{\mathbf{X}}^T \mathbf{P} \tilde{\mathbf{X}}$, where \mathbf{P} is symmetric positive semi-definite. The other part is the formation keeping error, i.e. $\sum_{i=1}^N (\tilde{\mathbf{X}}_i - \tilde{\mathbf{X}}_{i+1})^T \mathbf{Q} (\tilde{\mathbf{X}}_i - \tilde{\mathbf{X}}_{i+1})$, where \mathbf{Q} is symmetric positive semi-definite and i is defined modulo N . Matrix \mathbf{P} and \mathbf{Q} can be designed to adjust the relative weights of translational and rotational formation error based on certain requirements. Other functions are also feasible. We would like to design the non-linear gain matrices to meet the following requirements. When the spacecraft are out of the desired formation, that is, $E(\mathbf{X}, \mathbf{X}^d)$ is large, the virtual structure will slow down or even stop, allowing the spacecraft to regain formation. When the spacecraft are maintaining formation, that is, $E(\mathbf{X}, \mathbf{X}^d)$ is small, the virtual structure will keep moving toward its final goal at a reasonable speed. By this design, the virtual structure will be aimed at performing reasonably fast formation manoeuvres as well as preserving tight formation shape during the manoeuvre even in the case of control saturation, disturbances, and malfunctions. A candidate for such gain matrices can be defined as $\Gamma = \mathbf{K} + \mathbf{K}_F E(\mathbf{X}, \mathbf{X}^d)^2$, where $\mathbf{K} = \mathbf{K}^T > 0$ is the gain matrix which corresponds to the nominal formation speed when the formation is preserved tightly, and $\mathbf{K}_F = \mathbf{K}_F^T > 0$ is the formation gain matrix which weights the performance measure $E(\mathbf{X}, \mathbf{X}^d)$. In the case of $\mathbf{K}_F = 0$, no formation feedback is introduced. We will see that formation gain matrix with larger entries result in better formation maintenance but slower convergence speed. We can see that:

$$\begin{aligned}E(\mathbf{X}, \mathbf{X}^d) \rightarrow 0 & \Rightarrow \Gamma \rightarrow \mathbf{K} \\ E(\mathbf{X}, \mathbf{X}^d) \rightarrow \infty & \Rightarrow \Gamma \rightarrow \infty\end{aligned}$$

Correspondingly, non-linear gain matrix Γ_v , Γ_ω , and Γ_ξ in (7) can be defined as

$$\begin{aligned}\Gamma_v & = \mathbf{K}_v + \mathbf{K}_{Fv} E_v(\mathbf{X}, \mathbf{X}^d)^2 \\ \Gamma_\omega & = \mathbf{K}_\omega + \mathbf{K}_{F\omega} E_\omega(\mathbf{X}, \mathbf{X}^d)^2 \\ \Gamma_\xi & = \mathbf{K}_\xi + \mathbf{K}_{F\xi} E_\xi(\mathbf{X}, \mathbf{X}^d)^2\end{aligned}\quad (9)$$

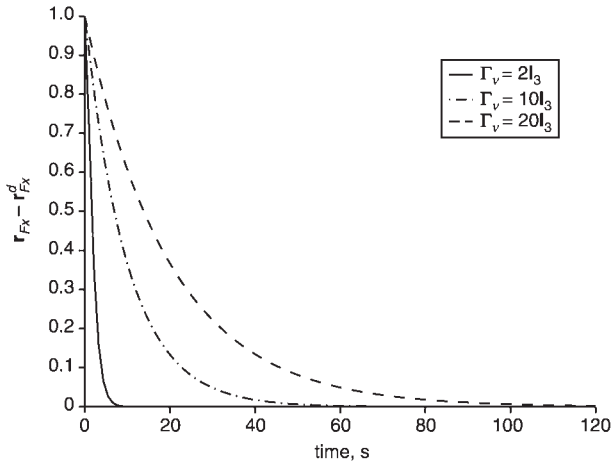


Fig. 2 Plot of $\tilde{\mathbf{r}}_{Fx}$ with initial conditions $\tilde{\mathbf{r}}_{Fx} = 1$ and $\dot{\tilde{\mathbf{r}}}_{Fx} = 0$ for different choices of Γ_v

where \mathbf{K}_v , \mathbf{K}_ω , \mathbf{K}_ξ , \mathbf{K}_{Fv} , $\mathbf{K}_{F\omega}$, and $\mathbf{K}_{F\xi}$ are symmetric positive definite matrices.

For a second order system $s^2 + k_1s + k_2 = 0$, if we define rise time t_r and damping ratio ζ , then natural frequency ω_n is approximately $1.8/t_r$. Therefore, if we let $k_2 = \omega_n^2 = (1.8/t_r)^2$ and $k_1 = 2\zeta\omega_n = 2\zeta(1.8/t_r)$, the transient specifications for the system are satisfied. We can design \mathbf{K}_r , k_q , \mathbf{K}_ξ , \mathbf{K}_{ri} , and k_{qi} according to k_2 , and design \mathbf{K}_v , \mathbf{K}_ω , \mathbf{K}_ξ , \mathbf{K}_{vi} , $\mathbf{K}_{\omega i}$ according to k_1 . For example, \mathbf{K}_r and \mathbf{K}_v can be defined as $k_2\mathbf{I}_3$ and $k_1\mathbf{I}_3$ respectively, where \mathbf{I}_3 is a 3×3 identity matrix.

Different designs for pairs (\mathbf{K}_r, Γ_v) , (k_q, Γ_ω) , and $(\mathbf{K}_\xi, \Gamma_\xi)$ can be applied to change the weights of translation, rotation, and expansion/contraction effects. As a result, non-linear gains slow down or speed up the virtual structure based on how far out of the desired formation the spacecraft are.

An illustrative example is shown as follows. Let $\mathbf{K}_v = \mathbf{I}_3$ and $k_p = 0$ in theorem 3.2. Note that the translational dynamics of the virtual structure can be rewritten as $\ddot{\tilde{\mathbf{r}}}_F + \Gamma_v \dot{\tilde{\mathbf{r}}}_F + \mathbf{K}_v \tilde{\mathbf{r}}_F$, where $\tilde{\mathbf{r}}_F = \mathbf{r}_F - \mathbf{r}_F^d = [\tilde{r}_{Fx}, \tilde{r}_{Fy}, \tilde{r}_{Fz}]^T$. Figure 2 shows a plot of \tilde{r}_{Fx} for different choices of matrix Γ_v . We can see that the dynamics of the virtual structure evolve more slowly as the elements of Γ_v are increased to be sufficiently large. That is, it takes a longer time for the virtual structure to achieve its desired states. When $\Gamma_v \rightarrow \infty$, the virtual structure will stop evolving.

When \mathbf{X}_F^d is specified for the virtual structure, $\mathbf{X}_F(t)$ will be regulated to \mathbf{X}_F^d according to the control law for the virtual structure with formation feedback. If the formation moves too fast, $E(\mathbf{X}, \mathbf{X}^d)$ will increase. As a result of the formation feedback, the virtual structure will slow down for the spacecraft to track their desired states, that is, to keep the formation. Thus $E(\mathbf{X}, \mathbf{X}^d)$ will decrease correspondingly, and the formation can keep moving toward its goal with a reasonable speed. As this coupled procedure proceeds with time, the formation manoeuvre will be asymptotically achieved.

3.2 Discussion

In the case of no formation feedback included, there is only uni-directional information flow from the virtual structure to each spacecraft, that is, the virtual structure does not need information from each spacecraft to evolve its dynamics. Also, each spacecraft derives its desired states based on the information from the virtual structure, that is, the received coordination vector \mathbf{X}_F . With formation feedback introduced, there is not only information flow from the virtual structure to each spacecraft but also information flow

from each spacecraft to the virtual structure. The centralised location where the coordination vector is implemented will need the information \mathbf{X}_i from each spacecraft, which requires more communication than the case without formation feedback.

Also note that even if those non-linear gain matrices are replaced by constant positive definite matrices, the proof for theorem 3.2 is still valid but there is no formation feedback included. However, without formation feedback included, how well the spacecraft will preserve the formation shape during the manoeuvre is not guaranteed. For example, the errors $\|\mathbf{r}_i(t) - \mathbf{r}_i^d(t)\|$ and $\|\mathbf{q}_i(t) - \mathbf{q}_i^d(t)\|$ for the i th spacecraft may be large during the manoeuvre due to control saturation or disturbances or even malfunctions, that is, the spacecraft may get out of the desired formation. If the virtual structure moves too fast, the spacecraft could fall far behind their desired positions or attitudes due to control saturation. If the virtual structure moves too slowly, the manoeuvre cannot be achieved within a reasonable time. In one extremal case, the virtual structure dynamics may evolve much faster than the spacecraft dynamics can achieve. When the virtual structure approaches its goal, each spacecraft tries to track the nearly constant desired states determined by \mathbf{X}_F^d , that is, transient performance during the manoeuvre is ignored. In the other extremal case, the virtual structure has to sacrifice its convergence speed significantly in order that each spacecraft can achieve good tracking performance, which result in unreasonably slow dynamics. Some spacecraft may also be perturbed by disturbances, which may cause them to be disintegrated from the desired formation. Without formation feedback, those disintegrated spacecraft will be left behind while the others keeping moving towards their goals, and the entire system cannot adjust to maintain formation. Therefore, we vary the non-linear gain matrices Γ_v , Γ_ω , and Γ_ξ with time to affect the evolution speed of the virtual structure according to the tracking performance of each spacecraft. As a result, formation feedback is introduced from the spacecraft to the virtual structure. This can be illustrated by the example in Section 3.1 and the simulation studies in the next Section.

Furthermore, to focus on the main issue, we assume that the dynamics of the virtual structure evolves much faster than the spacecraft dynamics when we introduce the non-linear gain matrices in the above discussion. In the case when the spacecraft are ahead of their desired configurations, it is straightforward to extend the above approach to speed up the virtual structure dynamics rather than slow it down. That is, the non-linear gain matrices can be designed to vary properly with regard to whether each spacecraft is ahead of or behind its desired configuration. For example, elements of the non-linear gain matrices can be increased or decreased based on whether the geometric centre of the spacecraft is behind or ahead of the virtual centre of the virtual structure.

4 Simulation results

In this Section we will consider a group of three spacecraft interferometers. The desired original positions of the three spacecraft are given by $\mathbf{r}_{1F}^d = [50, 0, 0]^T$, $\mathbf{r}_{2F}^d = [-50, 0, 0]^T$, $\mathbf{r}_{3F}^d = [0, 0, 50\sqrt{3}]^T$ metres and the desired original attitudes are given by $\mathbf{q}_{1F}^d = \mathbf{q}_{2F}^d = \mathbf{q}_{3F}^d = [0, 0, 0, 1]^T$ with respect to the formation frame \mathbf{C}_F . The three spacecraft will perform a formation manoeuvre of a combination of rotation and expansion from rest with some initial errors. The desired formation will start from rest with inertial attitude $\mathbf{q}_F(0) = [0, 0, 0, 1]^T$ to the desired inertial attitude $\mathbf{q}_F^d = [\mathbf{u}^T \sin(\pi/4), \cos(\pi/4)]^T$, where $\mathbf{u} = [0, 0, 1]^T$, and expand 1.5 times the original size.

The performance measure is chosen as $E(\mathbf{X}, \mathbf{X}^d) = \|\mathbf{X} - \mathbf{X}^d\|^2$. The parameters for each spacecraft and the virtual structure are given in Table 1 and Table 2 respectively, where \mathbf{I}_3 denotes the 3×3 identity matrix.

In simulation, we will plot absolute position and attitude errors as well as relative position and attitude errors for each

Table 1: Parameter values used in simulation for each spacecraft

Parameter	Value
M_i	150 kg
\mathbf{J}_i	$25\mathbf{I}_3$ kgm ²
\mathbf{K}_{r_i}	$0.81\mathbf{I}_3$
\mathbf{K}_{v_i}	$1.27\mathbf{I}_3$
k_{q_i}	3.24
\mathbf{K}_ω	$6.15\mathbf{I}_3$

Table 2: Parameter values used in simulation for the virtual structure

Parameter	Value
M_F	1 kg
\mathbf{J}_F	\mathbf{I}_3 kgm ²
\mathbf{K}_r	$0.03\mathbf{I}_3$
\mathbf{K}_v	$0.25\mathbf{I}_3$
k_q	0.05
\mathbf{K}_ω	$0.32\mathbf{I}_3$
\mathbf{K}_ξ	$0.03\mathbf{I}_3$
\mathbf{K}_ζ	$0.25\mathbf{I}_3$
\mathbf{K}_{Fv}	$0.01\mathbf{I}_3$
$\mathbf{K}_{F\omega}$	$0.02\mathbf{I}_3$
$\mathbf{K}_{F\xi}$	$0.01\mathbf{I}_3$
k_p, k_a, k_e	0

spacecraft. Control effort for some spacecraft will also be plotted. Absolute position error is represented by absolute difference between actual position and desired position for each spacecraft. Absolute attitude error is represented by absolute difference between actual attitude and desired attitude for each spacecraft. Since the formation shape is an equilateral triangle and the three spacecraft keep the same attitude in the formation, we use absolute difference between lengths of the sides in the equilateral triangle to represent the relative position error and absolute difference between the attitude of each spacecraft to represent the relative attitude error. If the formation is preserved exactly, the relative position and attitude errors should be zero.

In this Section, we use a subscript i ($1 \leq i \leq 3$) which is defined modulo 3 to represent the states for the i th spacecraft. For position and attitude error plots, in part (a), we plot absolute position errors represented by $\|\mathbf{r}_i - \mathbf{r}_i^d\|$. In part (b), we plot absolute attitude errors represented by $\|\mathbf{q}_i - \mathbf{q}_i^d\|$. In part (c), we plot relative position errors represented by $\|\|\mathbf{r}_i - \mathbf{r}_{i+1}\| - \|\mathbf{r}_{i+1} - \mathbf{r}_{i+2}\|\|$. In part (d), we plot relative attitude errors represented by $\|\mathbf{q}_i - \mathbf{q}_{i+1}\|$. For control effort plots, control force \mathbf{f} and control torque $\boldsymbol{\tau}$ will be plotted in parts (a) and (b) respectively. Note that sometimes, some curves may coincide with each other.

Two cases with and without formation feedback will be compared in this Section, including the case with control saturation and the case with control saturation and spacecraft failure.

Under control saturation, position and attitude errors without and with formation feedback are plotted in Figs. 3 and 4 respectively. Here we assume that the control force is saturated at $|f_x|, |f_y|, |f_z| = 50$ N and the control torque is saturated at $|\tau_x|, |\tau_y|, |\tau_z| = 0.3$ Nm. We can see that Fig. 4 achieves better performance than Fig. 3. Control effort for spacecraft #1 without and with formation feedback is plotted in Figs. 5 and 6 respectively. From Fig. 5, it is obvious that f_y saturates most of the time during the manoeuvre, which accounts for the bad formation-keeping performance shown in Fig. 3. However, in Fig. 6, f_y only

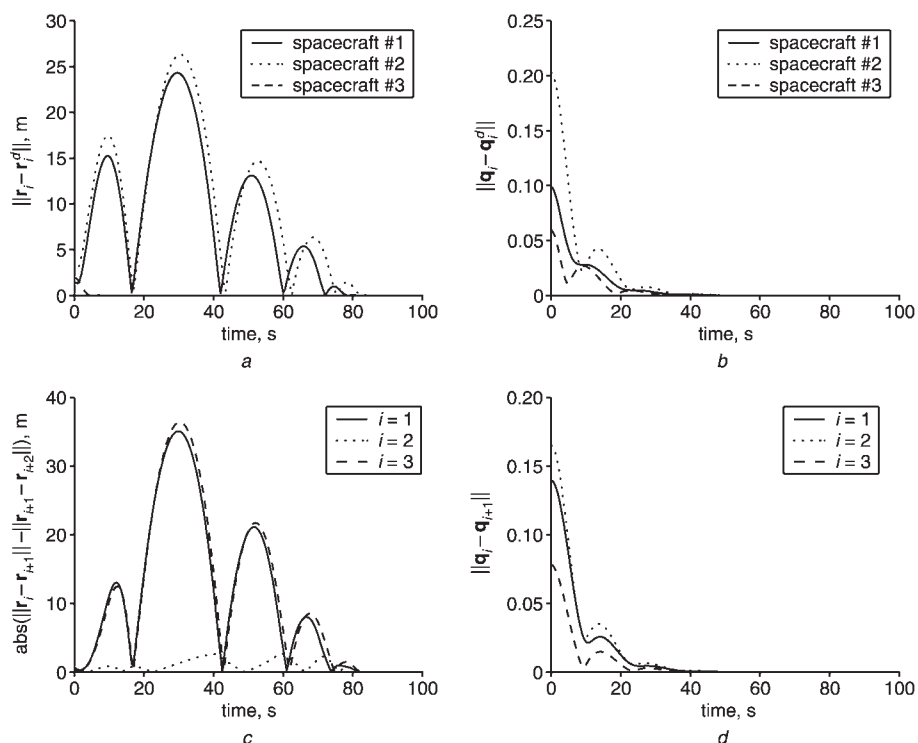


Fig. 3 Position and attitude errors under control saturation without formation feedback

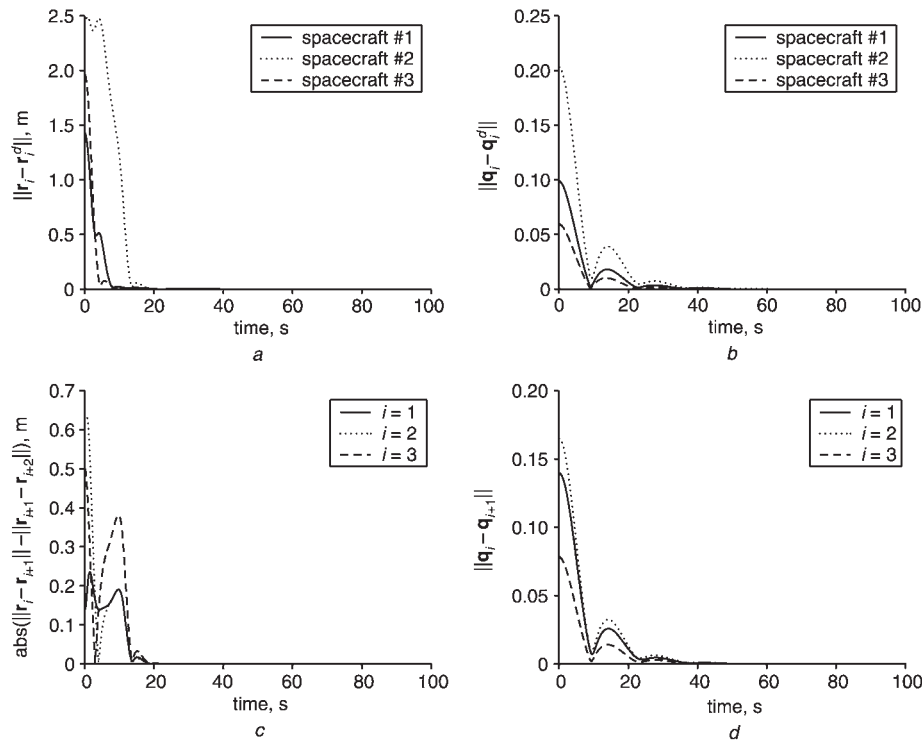


Fig. 4 Position and attitude errors under control saturation with formation feedback

saturates during the initial short time period due to the large initial errors.

In Figs. 7 and 8, we simulate the formation manoeuvre result under control saturation when spacecraft #1 fails from 5th to 20th second without and with formation feedback respectively. Since there is no formation feedback in Fig. 7, the virtual structure keeps moving towards its final goal even if one of the spacecraft fails for some time. As a result, spacecraft #1 cannot track its desired states satisfactorily, and the system has large absolute and relative errors during

the period when spacecraft #1 fails. The large absolute and relative errors after that period are due to the control saturation. In fact, in this case the spacecraft are out of formation for some time. However, in Fig. 8, since there is formation feedback, the virtual structure slows down to preserve the formation when one of the spacecraft fails for a period of time. As a result, the system in Fig. 8 has smaller absolute and relative errors than the one in Fig. 7. The control effort of the above two cases for spacecraft #1 is plotted in Figs. 9 and 10. We assume that spacecraft #1 has zero control

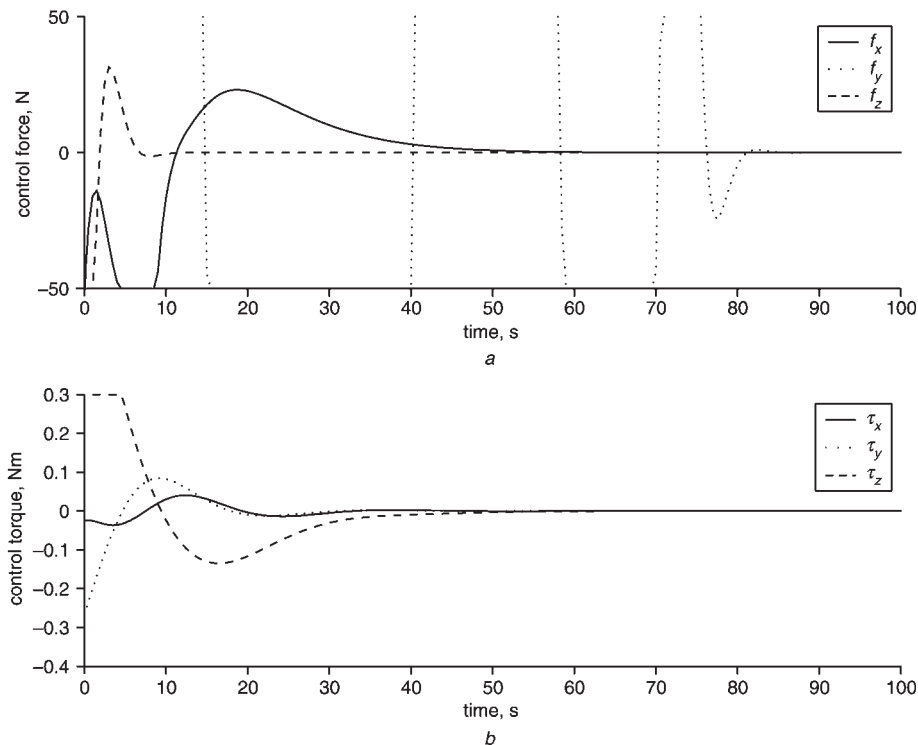


Fig. 5 Control effort for spacecraft #1 under control saturation without formation feedback

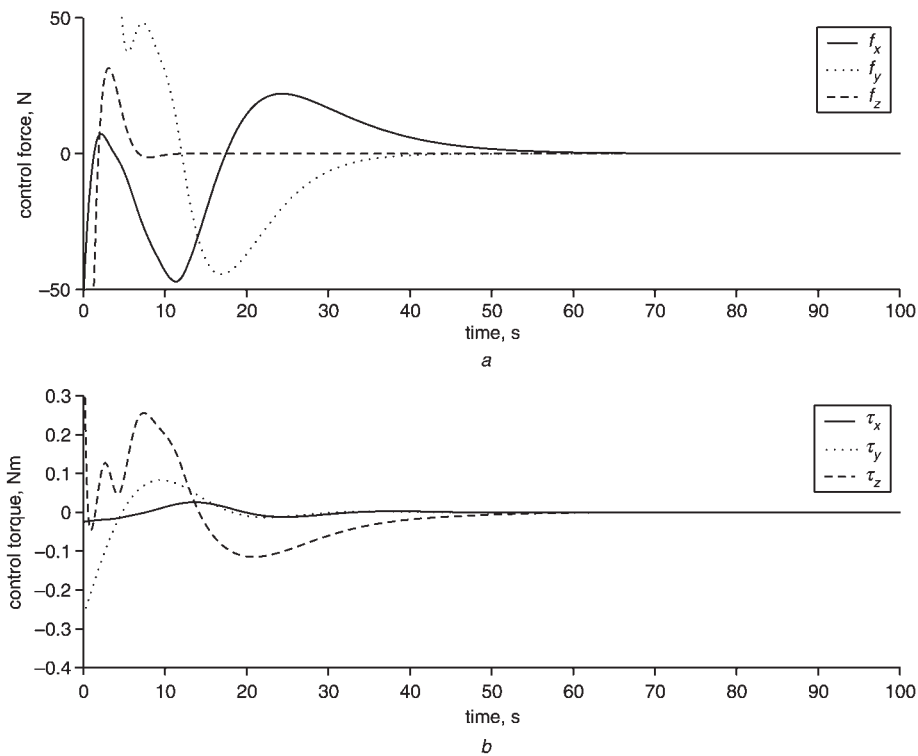


Fig. 6 Control effort for spacecraft #1 under control saturation with formation feedback

force and torque when it fails. Figure 9 shows that f_x and f_y for spacecraft #1 saturates most of the time, which is mitigated in Fig. 10 with formation feedback introduced.

Within the same range of error, the system with formation feedback can choose smaller rise time, and thus converge faster than the one without formation feedback. Within the same range of convergence speed, the system with formation feedback will have smaller errors than the one without formation feedback. Also, the system with formation feedback needs less control effort

for both cases. We know that absolute and relative errors and control efforts will decrease when the entries in the formation gain matrix \mathbf{K}_F increases, but the convergence speed will decrease correspondingly. At the same time, when the entries in the formation gain matrix \mathbf{K}_F decreases, the system will converge faster, but the absolute and relative errors and control efforts will increase correspondingly. We also know by simulation that it is hard to choose good rise times beforehand to achieve a good performance in the system without formation feedback. However, a wide

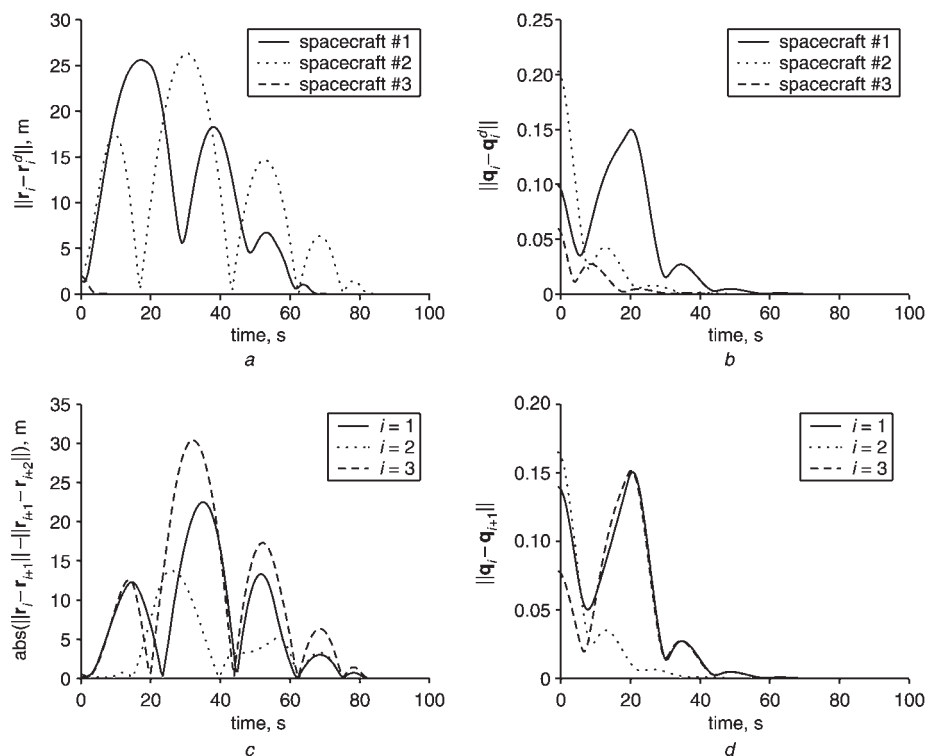


Fig. 7 Position and attitude errors under control saturation without formation feedback when spacecraft #1 fails for 15 seconds

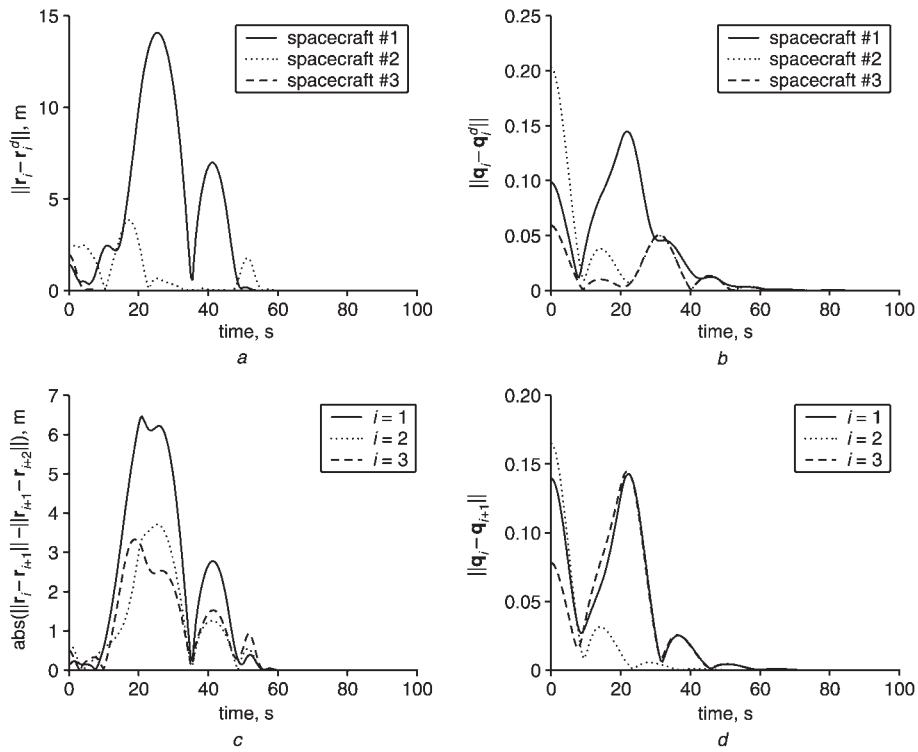


Fig. 8 Position and attitude errors under control saturation with formation feedback when spacecraft #1 fails for 15 seconds

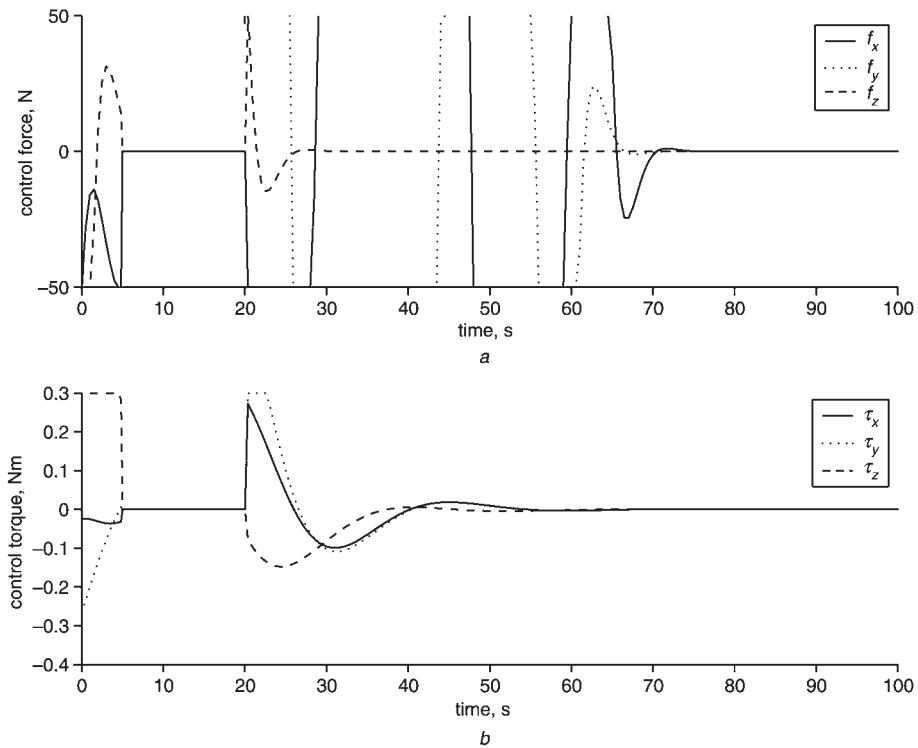


Fig. 9 Control effort for spacecraft #1 under control saturation without formation feedback when spacecraft #1 fails for 15 seconds

range of rise times work well in the system with formation feedback.

5 Conclusion

In this paper we have investigated an idea of introducing formation feedback under the framework of virtual structures through a detailed application of this idea to the problem of synthesising multiple spacecraft in deep space. From the simulation studies, we can see that introducing

formation feedback from spacecraft to the formation has several advantages. Firstly, the system can achieve a good performance in improving convergence speed and decreasing manoeuvre errors. Secondly, formation feedback adds a sense of group stability and robustness to the whole system. Thirdly, formation feedback improves the robustness with respect to choosing gains for different spacecraft. Finally, formation feedback makes formation-keeping more robust to synchronisation issues and the variability on each spacecraft.

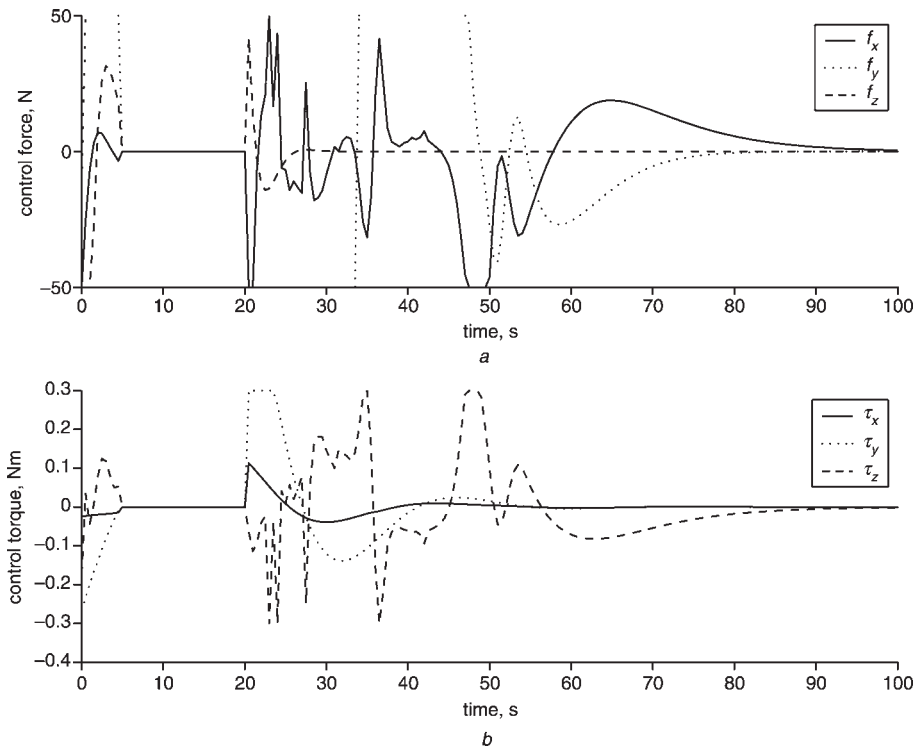


Fig. 10 Control effort for spacecraft #1 under control saturation with formation feedback when spacecraft #1 fails for 15 seconds

6 References

- 1 Wang, P.K.C.: 'Navigation strategies for multiple autonomous mobile robots moving in formation', *J. Robot. Syst.*, 1991, **8**, (2), pp. 177–195
- 2 Balch, T., and Arkin, R.C.: 'Behaviour-based formation control for multirobot teams', *IEEE Trans. Robot. Autom.*, 1998, **14**, pp. 926–939
- 3 Lewis, M.A., and Tan, K.-H.: 'High precision formation control of mobile robots using virtual structures', *Auton. Robots*, 1997, **4**, pp. 387–403
- 4 Fierro, R., Das, A., Kumar, V., and Ostrowski, J.: 'Hybrid control of formations of robots'. Proc. IEEE Int. Conf. on Robotics and Automation, Seoul, Korea, May 2001, pp. 157–162
- 5 Fax, J.A., and Murray, R.M.: 'Information flow and cooperative control of vehicle formations'. Presented at IFAC World Congress, Barcelona, Spain, 2002
- 6 Ogren, P., Egerstedt, M., and Hu, X.: 'A control Lyapunov function approach to multiagent coordination', *IEEE Trans. Robot. Autom.*, 2002, **18**, pp. 847–851
- 7 Wen, J.T.-Y., and Kreutz-Delgado, K.: 'The attitude control problem', *IEEE Trans. Autom. Control*, 1991, **36**, pp. 1148–1162
- 8 Kang, W., and Yeh, H.-H.: 'Co-ordinated attitude control of multi-satellite systems', *Int. J. Robust Nonlinear Control*, 2002, **12**, pp. 185–205
- 9 Giulietti, F., Pollini, L., and Innocenti, M.: 'Autonomous formation flight', *IEEE Control Syst. Mag.*, 2000, **20**, pp. 34–44
- 10 Stilwell, D.J., and Bishop, B.E.: 'Platoons of underwater vehicles', *IEEE Control Syst. Mag.*, 2000, **20**, pp. 45–52
- 11 Wie, B., Weiss, H., and Apaposthatis, A.: 'Quaternion feedback regulator for spacecraft eigenaxis rotations', *AIAA J. Guid. Control Dyn.*, 1989, **12**, pp. 375–380
- 12 Wang, P.K.C., and Hadaegh, F.Y.: 'Coordination and control of multiple microspacecraft moving in formation', *J. Astron. Sci.*, 1996, **44**, (3), pp. 315–355
- 13 Desai, J.P., Ostrowski, J., and Kumar, V.: 'Controlling formations of multiple mobile robots'. Proc. of IEEE Int. Conf. on Robotics and Automation, Leuven, Belgium, May 1998, pp. 2864–2869
- 14 Mesbahi, M., and Hadaegh, F.Y.: 'Formation flying control of multiple spacecraft via graphs, matrix inequalities, and switching', *J. Guid. Control Dyn.*, 2000, **24**, pp. 369–377
- 15 Lawton, J., and Beard, R.W.: 'Synchronized multiple spacecraft rotations', *Automatica*, 2000, **38**, (8), pp. 1359–1364
- 16 Schneider-Fontan, M., and Mataric, M.J.: 'Territorial multi-robot task division', *IEEE Trans. Robot. Autom.*, 1998, **14**, pp. 815–822
- 17 Parker, L.E.: 'ALLIANCE: An architecture for fault tolerant multirobot cooperation', *IEEE Trans. Robot. Autom.*, 1998, **14**, pp. 220–240
- 18 Beard, R.W., Lawton, J., and Hadaegh, F.Y.: 'A coordination architecture for formation control', *IEEE Trans. Control Syst. Technol.*, 2001, **9**, pp. 777–790
- 19 Leonard, N.E., and Fiorelli, E.: 'Virtual leaders, artificial potentials and coordinated control of groups'. Proc. of IEEE Conf. on Decision and Control, Orlando, Florida, December 2001, pp. 2968–2973

- 20 Skjetne, R., Moi, S., and Fossen, T.I.: 'Nonlinear formation control of marine craft'. Proc. IEEE Conf. on Decision and Control, Las Vegas, NV, December 2002, pp. 1699–1704
- 21 Hadaegh, F.Y., Lu, W.-M., and Wang, P.K.C.: 'Adaptive control of formation flying spacecraft for interferometry'. Presented at IFAC World Congress, 1998
- 22 Young, B., Beard, R., and Kelsey, J.: 'A control scheme for improving multi-vehicle formation manoeuvres'. Proc. American Control Conf., Arlington, VA, June 2001, pp. 704–709
- 23 Ren, W., and Beard, R.W.: 'Virtual structure based spacecraft formation control with formation feedback'. Presented at AIAA Guidance, Navigation, and Control Conf., Monterey, CA, August 2002
- 24 Hughes, P.C.: 'Spacecraft attitude dynamics' (John Wiley Sons, 1986)
- 25 Horn, R.A., and Johnson, C.R.: 'Matrix analysis' (Cambridge University Press, 1985)

7 Appendix

Euler's theorem for rigid body rotations states that "the general displacement of a rigid body with one point fixed is a rotation about some axis." Let \mathbf{z} represent a unit vector in the direction of rotation, called the eigenaxis, and let ϕ represent the angle of rotation about \mathbf{z} , called the Euler angle. The unit quaternion representing this rotation is given by $\mathbf{q} = [\mathbf{z}^T \sin(\phi/2), \cos(\phi/2)]^T = [\bar{\mathbf{q}}^T, \bar{q}]^T$, where $\bar{\mathbf{q}}$ is a 3×1 vector with its components represented in the given coordinate frame and \bar{q} is a scalar. It is easy to see that \mathbf{q} and $-\mathbf{q}$ represent the same attitude. However, uniqueness can be achieved by restricting ϕ to the range $0 \leq \phi \leq \pi$ so that $\bar{q} \geq 0$ all the time [24]. In the remainder of the paper, we assume that $\bar{q} \geq 0$.

Given a vector \mathbf{p} , the corresponding cross-product operation \mathbf{p}^\times is defined as

$$\mathbf{p}^\times = \begin{bmatrix} 0 & -p_3 & p_2 \\ p_3 & 0 & -p_1 \\ -p_2 & p_1 & 0 \end{bmatrix}$$

where $\mathbf{p} = [p_1, p_2, p_3]^T$ in terms of its components in the given coordinate frame.

If we let $\mathbf{C}_{O'O}$ be a rotation matrix that represents the orientation of the frame $\mathbf{C}_{O'}$ with respect to \mathbf{C}_O , then $\mathbf{r}_{O'} = \mathbf{C}_{O'O}\mathbf{r}_O$, where $\mathbf{r}_{O'}$ and \mathbf{r}_O represent vector \mathbf{r} in terms of its components in the frame $\mathbf{C}_{O'}$ and \mathbf{C}_O separately. The relationship between the unit quaternion \mathbf{q} and the rotation matrix \mathbf{C}_O is defined as [24]:

$$\mathbf{C}_{O'O} = (2\bar{q}^2 - 1)\mathbf{I} + 2\bar{\mathbf{q}}\bar{\mathbf{q}}^T - 2\bar{q}\bar{\mathbf{q}}^\times$$

The relationship between two rotation matrices $\mathbf{C}_{O'O}$ and $\mathbf{C}_{OO'}$ is given as:

$$\mathbf{C}_{OO'} = \mathbf{C}_{O'O}^T = (2\bar{q}^2 - 1)\mathbf{I} + 2\bar{\mathbf{q}}\bar{\mathbf{q}}^T + 2\bar{q}\bar{\mathbf{q}}^\times.$$

The multiplication of two quaternions is given by the formula $\mathbf{q}_a\mathbf{q}_b = \mathbf{Q}(\mathbf{q}_b)\mathbf{q}_a$, where

$$\mathbf{Q}(\mathbf{q}_b) = \begin{pmatrix} \bar{q}_b\mathbf{I} - \bar{\mathbf{q}}_b^\times & \bar{\mathbf{q}}_b \\ -\bar{\mathbf{q}}_b^T & \bar{q}_b \end{pmatrix}.$$

Let \mathbf{q}^* be the inverse of the quaternion \mathbf{q} given by

$$\mathbf{q}^* = \begin{pmatrix} \bar{\mathbf{q}} \\ \bar{q} \end{pmatrix}^* = \begin{pmatrix} -\bar{\mathbf{q}} \\ \bar{q} \end{pmatrix}.$$

Suppose that the unit quaternions \mathbf{q} and \mathbf{q}^d represent the actual attitude and the desired attitude of a rigid body respectively, then the attitude error is given by

$$\mathbf{q}_e = \mathbf{q}^*\mathbf{q}^d = \begin{pmatrix} \bar{\mathbf{q}}_e \\ \bar{q}_e \end{pmatrix}.$$